A 3.5-to-6.2-GHz Mixer-First Acoustic-Filtering Chipset with Mixed-Domain Asymmetric IF and Complex BB Recombination Achieving 170 MHz BW and +27 dBm IIP3 at 1×BW offset

Hyungjoo Seo, Mengze Sha, Jin Zhou University of Illinois at Urbana-Champaign, USA

Abstract — This paper presents a 3.5-to-6.2-GHz highlinearity mixer-first superheterodyne receiver chipset that utilizes gigahertz intermediate-frequency (IF) acoustic filters and a Weaver-like mixed-domain recombination architecture. The proposed mixed-domain recombination architecture enables a high IF (2.6 GHz) with a wide (170 MHz) instantaneous bandwidth (BW) and reduces the number of IF lossy passive components. Leveraging inherent quadrature down-conversion in the IF receiver, we adopt complex baseband signal processing to compensate in-phase and quadrature mismatch. Also, we identify that the IF integrated transformer loss is asymmetrical with respect to primary and secondary winding quality factors, and hence utilize stacked transformers for low loss and compact size. The chipset is fabricated using a 65-nm CMOS process and demonstrates, in measurement, an out-of-band IIP3 of +27 dBm at 1×BW offset with a 9.7-dB NF at 3.5-GHz RF.

Keywords — Receiver, mixer, BAW, filter, linearity, interference.

I. Introduction

With the advent of sub-6 GHz 5G and WiFi 6E, a mobile device needs to support tens of downlink bands with numerous front-end (FE) filters and switches which limit the system performance, cost, and size. The design of RF FE is expected to become more challenging with the trend towards MIMO, broadband, and dynamic spectrum access.

Mixer-first receivers [1], [2], [3], [4], [5] and high-order N-path filters [6], [7] have been proposed for monolithic reconfigurable RF FE. High-order N-path filters provide acoustic-filter-like selectivity at close-in offset frequencies but have limited tuning range and rarely operate above 2 GHz. Mixer-first receivers are widely tunable and have excellent out-of-band (OOB) linearity in the presence of blockers at far-out frequency offsets; however, they have limited suppression and linearity for close-in interference. In [8], a mixer-first acoustic-filtering FE was reported with superior rejection and OOB IIP3 at 1×BW offset while operating at 2.5-to-4.5-GHz RF, but it uses many off-chip components at intermediate frequency (IF) and only has an RF bandwidth (BW) of 65 MHz.

In this work, we present a 3.5-to-6.2-GHz mixer-first acoustic-filtering chipset with a 170 MHz RF BW that achieves +27 dBm IIP3 and >30 dB rejection at 1×BW offset, while having no off-chip components at IF other than acoustic filters. This is a 6-to-11-dB improvement in OOB IIP3 at 1×BW offset compared to mixer-first RXs in [1], [2], [3], [4], [5]. While the N-path filter in [6] has similar linearity performance, this work operates at 5× higher frequencies with 1.8× wider

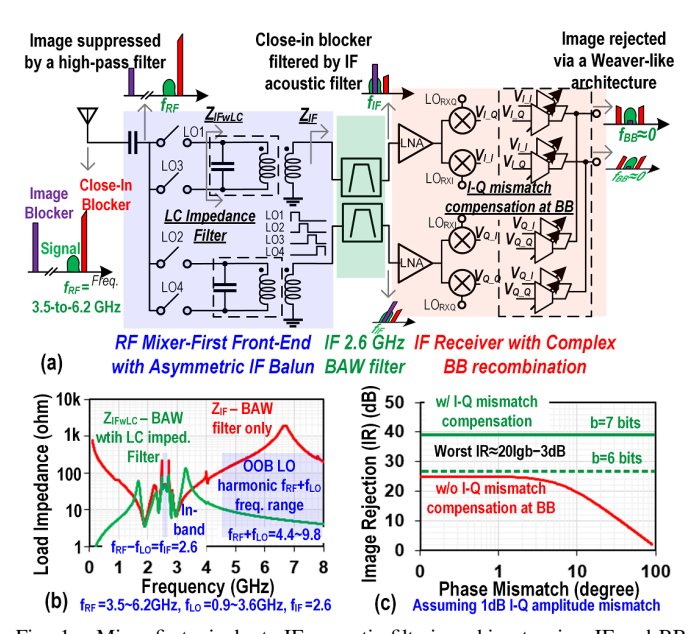


Fig. 1. Mixer-first gigahertz-IF acoustic-filtering chipset using IF-and-BB mixed-domain recombination: (a) concept; (b) mixer-first front-end LC loads suppress out-of-band impedance at LO harmonics, preventing impedance aliasing [8]; (c) image rejection with I-Q mismatch compensation at baseband.

tuning range and >15 dB higher OOB rejection. Compared to the mixer-first acoustic-filtering FE in [8], this work achieves 2.6× wider BW, operates at 1.4× higher RF, eliminates off-chip IF balun and inductor, while having comparable NF and linearity. These improvements are accomplished through a new mixer-first acoustic-filtering architecture, which (1) exploits a mixed-domain Weaver-like architecture, leveraging the frequency-independent 90° local oscillator (LO) for a higher IF and a wider BW, (2) utilizes baseband (BB) complex signal processing to compensate in-phase and quadrature (I-Q) mismatch, and (3) adopts a stacked IF transformer with a high coupling factor, reducing the loss and the occupied chip area.

II. ARCHITECTURE AND DESIGN CONSIDERATIONS

Unlike zero/low-IF mixer-first receivers (e.g. [1], [2], [3], [4], [5]), a gigahertz-IF superheterodyne architecture enables a mixer-first FE to use passive high-order acoustic filters at IF for superior linearity and selectivity. The key challenge associated with mixer-first acoustic-filtering is the presence of potential large IF impedances at OOB LO harmonics. All these OOB IF impedance components and the in-band impedance become indistinguishable, or aliases of one another, when

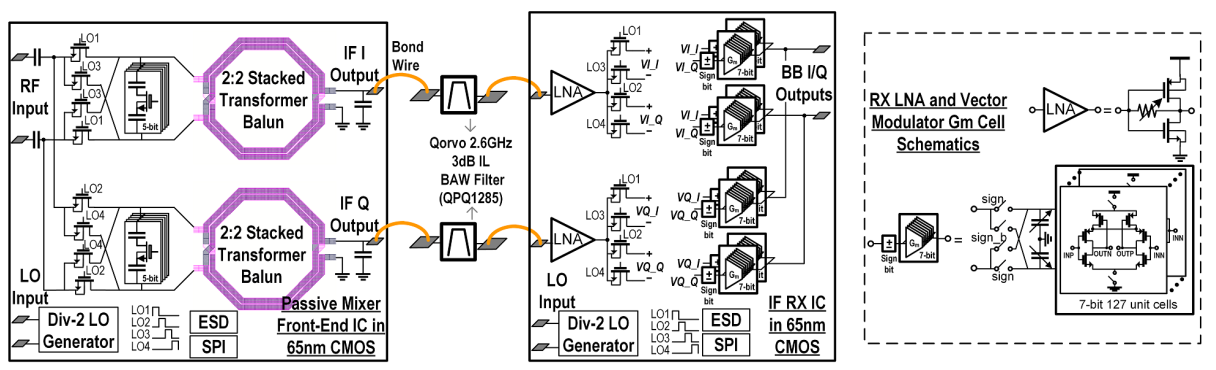


Fig. 2. Block diagram and schematic of our proposed mixer-first high-IF acoustic-filtering chipset with asymmetric IF and complex BB recombination.

translated to RF input via the passive-mixing operations; this impedance aliasing results in excess mixing loss and input impedance mismatch [8]. Following [8] and as shown in Fig. 1, we introduce an LC impedance filter that suppresses the IF load impedance at OOB harmonic frequencies, eliminating the excess loss and input impedance mismatch¹.

A. Mixed-Domain Recombination Architecture

In this work, we propose a new IF-and-BB mixed-domain recombination architecture for mixer-first acoustic filtering as shown in Fig. 1. A 4-path passive mixer driven by 25% duty-cycle non-overlapping clocks is followed by two *LC* impedance filters consisting of on-chip capacitors and transformer baluns at the in-phase and quadrature (I-Q) paths. These baluns also form the first-stage IF recombination that merges 4 paths into 2, halving the IF filter and receiver count. After the IF filters suppress strong OOB interference, a pair of IF quadrature direct-conversion receivers are adopted whose I-Q BB outputs are connected to act as the second-stage recombination at BB.

Our proposed IF-and-BB mixed-domain recombination enables a wider instantaneous BW and reduces the off-chip component count compared to the IF-only recombination in [8]. In an IF-only recombination network which is similar to the Hartley image-rejection architecture, a 90° phase shift and a signal summation are needed before the IF filter. To preserve the high linearity and compactness of the front-end, passive lumped phase shifter and combiner are needed (e.g. a lumped CLC phase shifter and a transformer balun were used in [8]), but this lumped passive network is intrinsically narrowband and often resorts to off-chip components for low loss (e.g. [7], [8]). In the proposed architecture, we push the narrowband phase shift and final stage recombination to the IF receiver and replace the signal-path phase shift with a frequency independent LO-path phase shift, leveraging receiver inherent 90° clocks. This leads to a broadband architecture without offchip and/or lossy IF passive components.

The benefits of our proposed architecture come at the expense of requiring one more IF acoustic filter and receiver. However, since only two *identical* acoustic filters are needed,

they can be fabricated together using the same process and hence have a significantly lower cost compared to having two acoustic filters at different frequencies [9]. In fact, it is essential to use two adjacent acoustic filters on the same die to reduce the I-Q mismatch in our architecture. The additional IF receiver does consume more power and chip area, but modern inductorless receivers in nanoscale CMOS processes are compact and power efficient.

Our proposed architecture resembles a Weaver imagerejection receiver but has two distinctions compared to prior works (e.g. [10]). Firstly, eliminating the RF low-noise amplifier and utilizing a mixer-first design significantly enhances the front-end dynamic range. Secondly, the choice of a gigahertz IF allows us to use high-linearity passive acoustic filters to replace active filters; also, a gigahertz high IF leads to a wide frequency separation between the image band and the desired signal band, easing the design of a high-pass image filter.

B. Complex BB Recombination

One challenge in our architecture is the I-Q mismatch which leads to degraded image rejection. While it has been shown that image rejection can be obtained in the digital domain [11], an image-band blocker could stress the dynamic range requirement of the front-end and saturate the receiver.

I-Q imbalance arises from RF and IF mixers and their associated LO signals are frequency independent [10]. To compensate this frequency-independent amplitude-and-phase mismatch, we utilize a complex BB recombination, as shown in Fig. 2, which includes a 7-bit vector modulator at each IF receiver I or Q BB output. The outputs of the vector modulators are added in the current domain for high linearity in the presence of image-band blockers. It can be shown that the 7-bit vector modulators can compensate a wide range of I-Q amplitude and phase mismatches with a worst-case image rejection of around 40 dB [see Fig. 1(c)].

Frequency-dependent I-Q imbalance is dominated by the mismatch between the two IF acoustic filters. Our proposed complex BB recombination can also compensate this I-Q imbalance across a finite BW, suppressing image band blockers.

C. Asymmetric IF Transformer Balun

While simultaneously acting as parts of the LC impedance filter and the IF recombination, the on-chip transformer baluns

¹Only the most significant OOB harmonic $f_{RF} + f_{LO}$ is shown in Fig. 1(a).

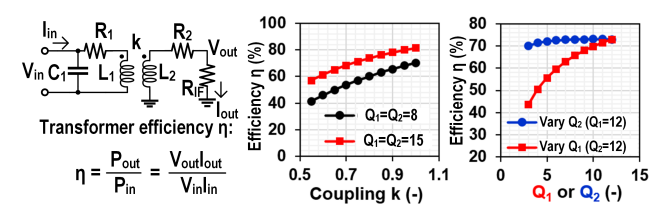


Fig. 3. IF transformer balun efficiency is asymmetrical between the primary and secondary winding Q factors, and the efficiency is mostly determined by the primary Q_1 . ($L_1=L_2=2$ nH, $R_{IF}=100~\Omega$, $f_{IF}=2.6$ GHz)

could introduce significant loss in practice, desensitizing the receiver front-end. We have derived the transformer loss or efficiency analytically using a simplified model as in Fig. 3. The efficiency can be calculated

$$\eta = \left(1 + \frac{\omega_{IF}L_2}{Q_2R_{IF}} + \frac{1}{k^2} \frac{R_{IF}}{Q_1\omega_{IF}L_1}\right)^{-1},\tag{1}$$

where $Q_i=\frac{\omega_{IF}L_i}{R_i},\ i=1$ or 2, and we've assumed C_1 resonates with the inductive component at IF.

Based on (1), a low-loss or high-efficiency transformer requires high Q and coupling factors. However, there exists a trade-off between Q and coupling factors in integrated transformers. A coplanar transformer features high Q but has limited coupling. A stacked transformer has strong coupling but uses a lower thin metal layer, degrading the Q factor.

Interestingly, based on (1) we find that the transformer efficiency is asymmetrical between the primary and secondary winding Q factors, and the efficiency is mostly determined by the primary Q_1 (see Fig. 3). Based on this insight, we adopt a 2:2 stacked transformer achieving a high coupling around 0.9. The top thick metal is assigned to the primary resulting in a Q of 13.8 with 0.8 dB loss at 2.6 GHz IF while the secondary has a Q of 5.6 and a loss of 0.3 dB.

III. IMPLEMENTATION AND MEASUREMENT RESULTS

Figure 2 depicts the block diagram and schematic of the FE mixer and IF receiver chipset in 65 nm bulk CMOS with two 2.6-GHz Qorvo QPQ1285 BAW filters. FE mixer switches are designed with on-resistance of 5Ω . Both the primary and secondary windings of IF transformers have inductance of 2 nH for a balance between area and power loss. At each FE balun output, an on-chip capacitor and a 2-mm bond wire form an L matching network further boosting the IF load impedance. As to the IF receiver, each I/Q path consists of a resistive feedback LNA followed by a 4-phase passive mixer. A clock generation circuit is shared among two receiving paths.

The fabricated chips, shown in Fig. 4, are packaged in QFN and mounted on a FR-4 PCB with the two 2.6-GHz BAW filters. A 1:1 SMD balun is used to facilitate single-ended measurements and its loss has been de-embedded.

The measured conversion gain, input matching, and NF are plotted in Fig. 5 with BAW filter S parameters, when RF input is tuned at 3.5 GHz with FE LO at 0.9 GHz. This frequency setting corresponds to the closest image and signal bands separation of 1.8 GHz. Across the range of 3.5 to 6.2 GHz, this separation varies from 1.8 to 5.2 GHz. The filtering chipset has

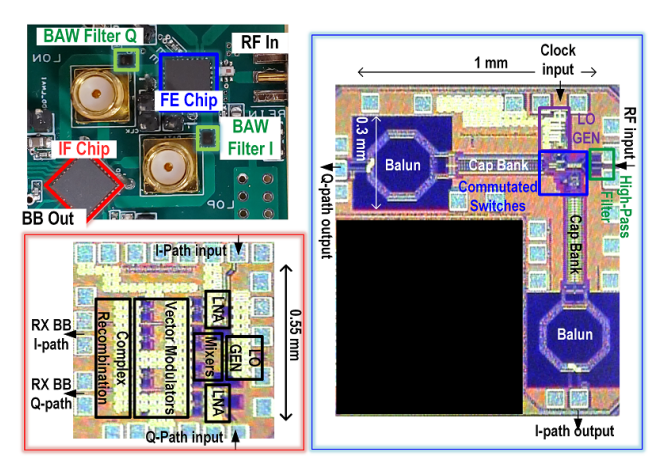


Fig. 4. Mixer-first acoustic-filtering chipset on a PCB with CMOS die photos.

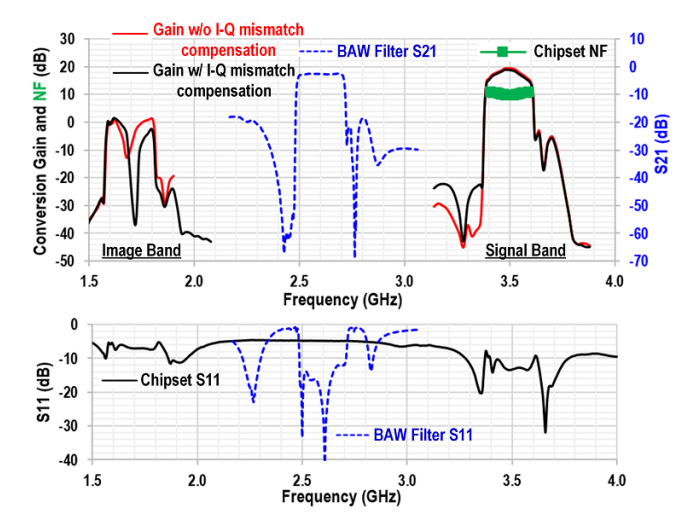


Fig. 5. Measured chipset gain, NF, and input matching (S11) at 3.5 GHz. Two gain results are plotted: one (red) with a nominal BB vector modulator setting assuming no I/Q mismatch and the other (black) with vector modulators exercised to compensate I/Q mismatch, hence maximizing image rejection.

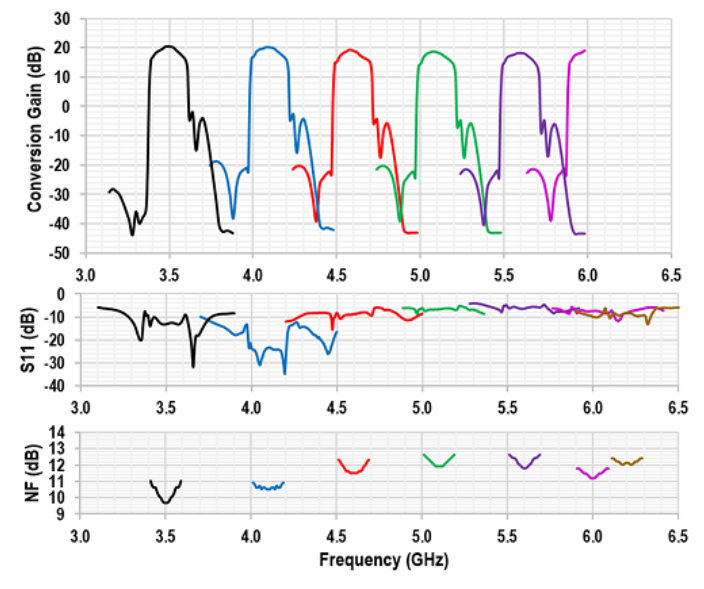


Fig. 6. Measured chipset gain, NF, and S11 across 3.5-to-6.2-GHz RF range.

Table 1. Measurement summary and comparison with state-of-the-art works	Table 1.	Measurement summary	v and	comparison	with	state-of-the-art wor	ks.
---	----------	---------------------	-------	------------	------	----------------------	-----

	RFIC 2018 [4]	JSSC 2018 [5]	JSSC 2020 [1]	JSSC 2020 [2]	JSSC 2019 [6]	ISSCC 2013 [10]	RFIC 2020 [8]	This work
RF Range (GHz)	2 to 8	0.2 to 8.0	0.2 to 2	0.5 to 2	0.8 to 1.1	~1.96	2.5 to 4.5	3.5 to 6.2
IF (MHz)	0	0	0	0	N/A	30	1600	2600
3dB RF BW (MHz)	80	20	18	260	30 to 50	5	65	170
NF (dB)	10 to 12	3.5 to 7.1	4.3 to 7.6	5.5	5.0 to 8.6 (FE only)	4.5	5.5 to 7.1 (FE only)	9.7 to 12 (FE + RX)
Rejection @ 1×BW _{RF}	10 to 15 dB	15 to 20 dB	14 dB	25 dB	10 to 15 dB	N/A	45 to 55 dB	30 to 45 dB
OOB-IIP3 @ 1×BW _{RF}	+21 dBm	+16 dBm	+15 dBm	+16 dBm	+24 dBm	0 dBm	+29.4 dBm	+27 dBm
B-1dB @ 1×BW _{RF}	+2 dBm	0 dBm	-3 to +5 dBm	-4.4 dBm	+9 dBm	-20 dBm	+4.3 dBm	+5 dBm
Power (mW)	1466 + 656 (RF + BB)	56 to 290	147 to 179	26 to 37	80 to 97 (FE only)	155	12 to 26 (FE only)	28 to 48 + 62 (FE + RX)
Silicon Technology	130-nm BiCMOS	45nm CMOS	28nm CMOS	28nm CMOS	65nm CMOS	65nm CMOS	65nm CMOS	65nm CMOS
Chip Area (mm²)	3.4 + 5 (RF + BB)	0.8	0.48	0.16	1.9 (FE only)	~1	1.4 (FE only)	0.5 + 0.35 (FE + RX)
Off-Chip Component	none	RF balun	none	RF balun	RF balun	RF balun	RF and IF baluns, IF inductor, SAW filters	RF balun, BAW filters
Direct-Conversion Mixer-First FE		FE 💳	High-Order N-Path Filter		Superheterodyne receiver and FE		N/A: not applicable	

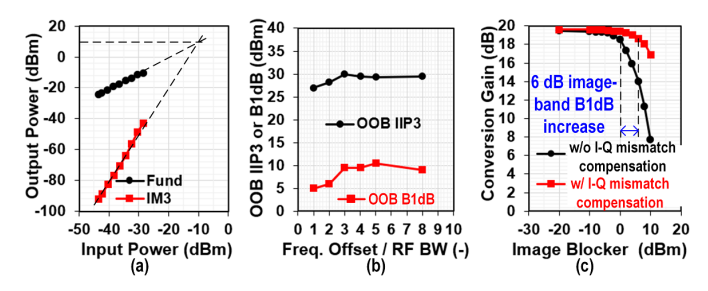


Fig. 7. Measured linearity performance: (a) in-band IP3, (b) OOB IIP3 and B1dB, and (c) image-band B1dB.

a conversion gain of 20 dB, minimal NF of 9.7 dB, and a 3-dB RF BW of 170 MHz. This NF consists of 3.7 dB mixer loss, 3 dB filter loss, and 3 dB RX NF; all package and bond wire losses are included. The RF BW is slightly reduced from filter 196-MHz BW due to mixer *LC* load and receiver BB filtering but they provide more far-out suppression. 33 dB image rejection is measured with mixed-domain recombination. When the vector-modulator-based complex recombination is enabled, an additional 25 dB rejection (58 dB total) is obtained. More image rejection across a wider BW may be obtained in the digital domain [11] or by a high-pass filter at the RF input.

The measured performance across 3.5-to-6.2 GHz RF is depicted in Fig.6 with 17-to-20 dB conversion gain, 9.7-to-12 dB NF, >30 dB rejection at 1×BW offset. Due to our input balun PCB design, the S11 beyond 4.5 GHz is degraded.

The measured linearity results with RF tuned at 3.5 GHz show an in-band OIP3 of +10 dBm [Fig. 7(a)] and OOB IIP3 of +27 dBm at 1×BW offset [Fig. 7(b)]. In the presence of an image single-tone blocker at 1.7 GHz, our complex BB recombination enhances the B1dB by 6 dB as shown in Fig. 7(c). This increase is accomplished through improved image rejection after compensating I-Q mismatches mentioned in Section II-B and shown in Fig. 5.

Compared to prior works (Table 1), this work concurrently achieves superior linearity and filtering at close-in offset, >160 MHz instantaneous RF BW, and operates above 2 GHz.

IV. CONCLUSION

We have demonstrated a mixer-first acoustic-filtering chipset operating at critical sub-7-GHz frequencies from 3.5 to 6.2 GHz while achieving 9.7-to-12-dB NF, 170 MHz instantaneous BW, and +27 dBm OOB IIP3 at 1×BW offset. These have been accomplished through a new mixer-first

acoustic-filtering architecture, which (1) exploits a mixed-domain Weaver-like architecture, leveraging the frequency-independent 90° LO for a high IF and a wide BW, (2) utilizes BB complex signal processing to compensate I-Q mismatch, and (3) adopts a stacked IF transformer with a high coupling factor, reducing the loss and the occupied chip area. Future works include integration of an RF high-pass filter to further suppress image blockers, reduction of I-Q mismatch via a same-wafer adjacent acoustic filter pair, and scaling operation frequency into millimeter-wave frequency bands.

ACKNOWLEDGMENT

We thank NSF SpecEES program for support.

REFERENCES

- [1] S. Krishnamurthy and A. M. Niknejad, "Design and Analysis of Enhanced Mixer-First Receivers Achieving 40-dB/decade RF Selectivity," IEEE J. Solid-State Circuits, vol. 55, no. 5, pp. 1165–1176, 2020.
- [2] G. Pini, D. Manstretta, and R. Castello, "Analysis and Design of a 260-MHz RF Bandwidth +22-dBm OOB-IIP3 Mixer-First Receiver With Third-Order Current-Mode Filtering TIA," *IEEE J. Solid-State Circuits*, vol. 55, no. 7, pp. 1819–1829, 2020.
- [3] P. K. Sharma and N. Nallam, "Breaking the Performance Tradeoffs in N-Path Mixer-First Receivers Using a Second-Order Baseband Noise-Canceling TIA," *IEEE J. Solid-State Circuits*, pp. 1–1, 2020.
- [4] E. C. Szoka and A. Molnar, "Circuit Techniques for Enhanced Channel Selectivity in Passive Mixer-First Receivers," in *IEEE Radio Frequency Integrated Circuits Symposium (RFIC) Dig.*, 2018, pp. 292–295.
- [5] Y. Lien, E. A. M. Klumperink, B. Tenbroek, J. Strange, and B. Nauta, "Enhanced-Selectivity High-Linearity Low-Noise Mixer-First Receiver With Complex Pole Pair Due to Capacitive Positive Feedback," *IEEE J. Solid-State Circuits*, vol. 53, no. 5, pp. 1348–1360, 2018.
- [6] P. Song and H. Hashemi, "RF Filter Synthesis Based on Passively Coupled N-Path Resonators," *IEEE J. Solid-State Circuits*, vol. 54, no. 9, pp. 2475–2486, 2019.
- [7] N. Reiskarimian and H. Krishnaswamy, "Design of all-passive higher-order CMOS N-path filters," in *IEEE Radio Frequency Integrated Circuits Symposium (RFIC) Dig.*, 2015, pp. 83–86.
- [8] H. Seo and J. Zhou, "A 2.5-to-4.5-GHz Switched-LC-Mixer-First Acoustic-Filtering RF Front-End Achieving <6dB NF, +30dBm IIP3 at 1 x Bandwidth Offset," in *IEEE Radio Frequency Integrated Circuits Symposium (RFIC) Dig.*, 2020.
- [9] A. Hagelauer, G. Fattinger, C. C. W. Ruppel, M. Ueda, K. Hashimoto, and A. Tag, "Microwave Acoustic Wave Devices: Recent Advances on Architectures, Modeling, Materials, and Packaging," *IEEE Trans. Microw. Theory and Techn.*, vol. 66, no. 10, pp. 4548–4562, 2018.
- [10] L. Sundstrom, M. Anderson, R. Strandberg, S. Ek, J. Svensson, F. Mu, T. Olsson, I. u. Din, L. Wilhelmsson, D. Eckerbert, and S. Mattisson, "A receiver for LTE Rel-11 and beyond supporting non-contiguous carrier aggregation," in *IEEE Int. Solid-State Circuits Conf. (ISSCC) Dig. Tech.* Papers, 2013, pp. 336–337.
- [11] S. Hwu and B. Razavi, "An RF Receiver for Intra-Band Carrier Aggregation," *IEEE J. Solid-State Circuits*, vol. 50, no. 4, pp. 946–961, 2015.